Engineering and Technology Journal
Journal homepage: https://etj.uotechnology.edu.iq

Investigation of Offshore Wind Turbine Structure Deflection Using Experimental Work, Numerical, and Theoretical Approach

Hayder M. Ali [a*], Hassan M. Alwan[a], Israa Al-Esbe[a], Kochneva O. V[b]

[a] Mechanical Engineering Dept., University of Technology-Iraq, Alsina'a street, 10066 Baghdad, Iraq.
[b] Peter the Great Saint Petersburg Polytechnic University, Russian Federation.
*Corresponding author Email: me.19.17@grad.uotechnology.edu.iq

HIGHLIGHTS

- One of the reasons for the low efficiency of offshore wind turbines in generating electricity is due to the deflection of the turbine support structure, due to the structure's exposure to the combined dynamic loads of the wind and seawater wave. Thus, knowing the extent to which the proposed structure of the study succeeds or fails.

ARTICLE INFO

Handling editor: Sattar Aljabair

Keywords:
Monopile; Offshore wind turbine (OWT); Deflection; Computational Fluid Dynamics (CFD); ANSYS-Fluent.

ABSTRACT

Electrical energy from offshore wind turbines is an important source of clean, renewable energy production. One of the reasons for the low efficiency of wind turbines is the change in the flow angle of attack, denoted by the symbol (α), as a result of the deflection of the structure. The study aims to know the values of the maximum deflection of the proposed structure under the environmental conditions of the Arabian Gulf water area. Our research adopted a novel approach to extracting results; the characteristics of sea waves were extracted from the experimental work after fixing five sea waves, knowing the displacement of the top of the structure, and using the numerical approach in the ANSYS-Fluent program to know the average wind and wave forces. Two simulations were performed. The first included the five cases of sea wave characteristics without rotating wind turbine blades. The second was for the fifth case only with the wind turbine blades rotating at a speed of (20.5 rpm), assuming that the structure was exposed to a constant wind speed (12 m/s) for the two simulations. The study also included obtaining the maximum deflection value of the structure. Then, the equations of the theoretical approach were developed based on the Euler-Bernoulli bending moment equation, and the forces extracted from the simulations were entered into the theoretical equations to extract the maximum deflection values of the structure. Reading the experimental work resulted in the highest displacement of the top of the structure in the fifth case (0.178 m). The result of the second simulation had the highest value of the structure deflection (0.201 m). In comparison, its value came in the theoretical approach (0.160 m), which adopted the forces of the second simulation.

1. Introduction

To keep up with social and economic development and improve people's well-being and health, demand for energy and related services is rising. Since around 1850, global consumption of fossil fuels (coal, oil, and gas) has expanded to the point where they now dominate the energy supply, resulting in rapid increases in carbon dioxide emissions. As a result, energy scientists and specialists have resorted to adopting vital and useful solutions for human communities to provide clean electric energy that does not contaminate the environment.

Offshore wind energy technologies have a larger potential for technological improvement in the future. Although wind energy is variable and, to some extent, unpredictable, experience and comprehensive research from various places have shown that wind energy integration does not have intractable technical repercussions.

The first big offshore wind farm (farm Horns Rev) off the Danish coast was created in the North Sea (farm Horns Rev) in 2002, thinking the winds above sea level were faster and steadier [1]. Specialists in the field of sustainable energy production from wind turbines have invented new ideas in the last four decades, including establishing wind turbine farms in the sea. They were initially close to the beaches with different support foundations, the most important of which were (Gravity base

http://doi.org/10.30684/etj.2022.133645.1199
Received 21 April 2022; Accepted 07 August 2022; Available online 13 October 2022
2412-0758/University of Technology-Iraq, Baghdad, Iraq

structure, Jacket structure, Tripod structure, and monopile structure), as shown in Figure (1). The most common and used is the type of monopile, where the percentage of its use in this field is about 60% [2].

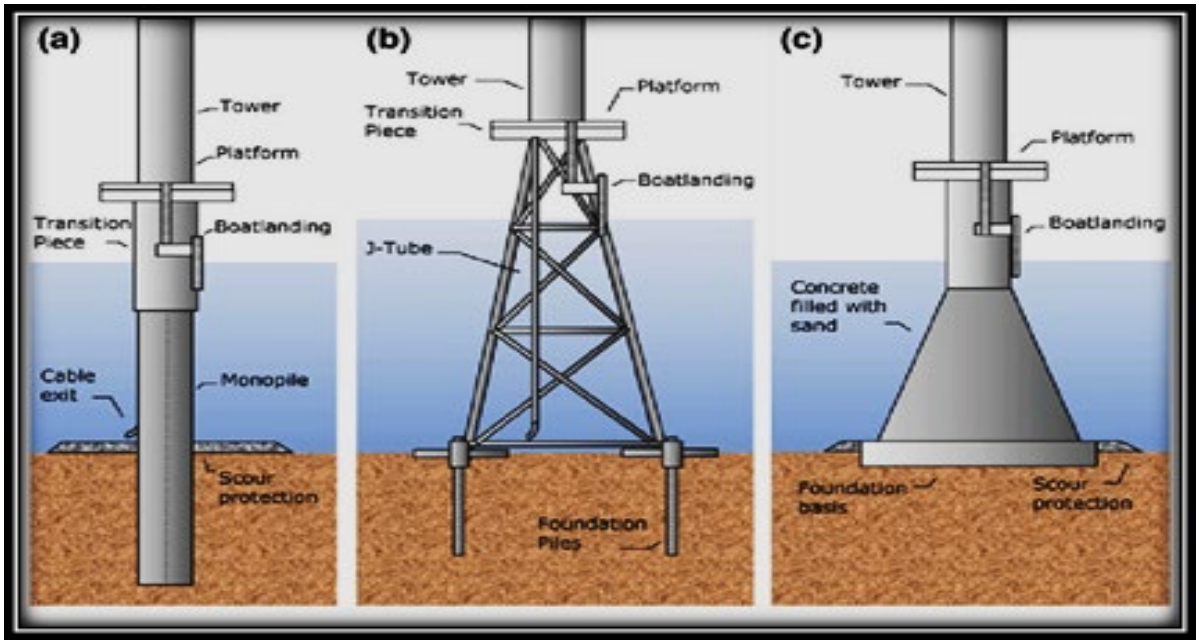

Figure 1: Shows the three types of turbine foundations: (a) monopile, (b) jacket, and (c) gravity based [3]

Offshore wind turbine support structures face harsh environmental conditions due to their exposure to the combined loads of wind and sea waves, which leads to the occurrence of stresses and moments in the structure, including bending moments.

The bending moment of the structure fixed at one end and the other free leads to the displacement of the structure from its original vertical axis at a certain angle. Thus, the deflection may lead to the failure of the structure or negatively affect the turbine's generation of electricity as a result of changing the angle of attack of wind with the wind turbine blades if the deflection is greater than the value of the permissible deflection of the structure and its amount (0.338 m). ANSYS-Fluent is a fluid simulation software known for its advanced physics modeling capabilities and accuracy. It is the most powerful computational fluid dynamics tool and includes well-validated physical modeling capabilities to deliver fast, accurate results [4]. The program was used to obtain numerical approximation solutions to the differential or integral-differential equations. The aerodynamic condition on the blades of the turbine was described, as well as the description of the air loads on the tower and hydrodynamic loads on the submerged structure. By imposing correct estimates on small areas in space or time, the numerical solution will provide results in separate areas in space and time and provide the values of the forces and their distribution on the structure under study. In 2013 Chen, Da et al. presented an article that investigated the structural properties of the supporting structures of monopile and tripod wind-turbine support structures [5].

Concerning increases in wave height and combined loading, offshore wind turbine (OWT) support structures are subjected to non-proportional environmental wind and wave load patterns. For all of the above, in 2014, Wei, Kai et al. proposed the Incremental Wind Wave Analysis (IWWA) for the structural capacity of WOW support structures [6]. In 2015, Dan Kallehave et al. studied how modern optimization approaches can be applied to monopile wind turbine support structures and identified key drivers where novelty in high-precision engineering approaches can impact the next generation of monopile. [7] In 2015 Kai Wei et al. presented a paper that assessed the structural integrity of jacket-supported offshore wind turbines under severe environmental loading conditions. They based their approach on a static rheological analysis of the jacket-type supporting structure subject to combined wind and wave load patterns [8]. Israa Al-Esbe et al. studied the erratic flow activity of HAWTs in two cases in 2016. The rotor was the first example. The rotor with the tower was the second case, which was solved using a panel method and a RANSE method [9]. In 2016, Samal, Ashis Kumar S et al. presented a study on how deflection and stress were distributed in a long, thin cantilever bundle with a regular rectangular cross-section and linear and homogenous elastic material characteristics. [10] In 2016 Arshad, Muhammad et al. presented a recent review paper on the engineering design, nominal size, and structural and environmental loading of existing, planned, and mono-founded OWT structures [11]. In 2016 Dymarski, Pawel et al. presented a research paper describing an effective method for determining wave and current loads acting on the supporting structures of offshore wind turbines. The CFD simulations were run for a defined range of period variation and a specific range of velocity amplitudes. The simulations were carried out in the time domain, yielding a force distribution function along the construction elements. The forces coefficients were comparable to the values determined experimentally by Sarpkaya [12, 13]. Based on the findings of the CFD study of segments of similar shape to a cylinder [14]. In 2020 Lokesh Ram, S. et al. published a paper about using Finite Element Analysis (FEA) to evaluate the deformation, stresses, and energy strain of a monopile structured Offshore Wind Turbine (OWT) and its tower (OWT) in thick sand [15]. In the year 2020, Alwan et al. conducted research on the analysis of wave intensity on the foundation of a mono-surface offshore wind turbine (NREL 5 megawatts), with the foundation chosen in the middle water region with a water depth of 25 meters. [16] In 2020, Sajjad tested two fixed-type foundations, one of them is monopile, and the other is a jacket [17]. Using (p–y)

curves, in 2020, Zhaoyao Wang et al. researched rigorously controlling the displacement of monopile offshore wind turbines, not ignoring the influence of local scour [18]. In 2021, Jianhua Zhang et al. suggested a method for the dynamic response of offshore structures by combining segmented responses is proposed, which depends on the pole-residue method to calculate those segmented responses. Numerical results show that the estimated displacement from the proposed method is consistent with the analytical result. The computational time required to obtain poles and residues of the loading is significantly reduced compared to the traditional pole-residue method. The developed approach is less sensitive to the adopted time interval than numerical approximation procedures [19]. In 2021, Mallikarjun et al. mainly focused on designing a wind tower for Uttar Kannada, the Western Ghats of Karnataka State, which is one of the potential sources of wind energy. The main objective is to find high-strength material for wind turbine towers. The geometric design of the 2MW power generation wind turbine tower is carried out in CATIA V5 and analyzed in ANSYS Workbench 19.2 for structural steel, Alloy steel 4130, and Alloy steel 6150 materials. Structural analysis, model analysis, fatigue life estimation, and validation of the results were performed. They then concluded from the results that Alloy steel 6150 is safe and economical to design compared to other materials.[20] In 2022 Gao, Zhi-Teng et al. published a brief paper outlining research into the effectiveness and security of offshore wind farms. To thoroughly grasp the significant issues with hydrodynamics for offshore wind turbines, the essay examined hydrodynamics, aerodynamics, structural dynamics, and resilience [21]. In 2022, Andrija Buljac et al. conducted a study that focused on manipulating the effects of environmental load on offshore wind turbines concurrently exposed to wind, waves, and currents in the form of small-scale laboratory experiments in a wind, wave, and Current Reservoir (WWCT) at Newcastle University, UK, using a scale model of offshore wind turbines. Higher amplitude waves cause an increase in the relative standard deviation of the integral loads, an effect that is more pronounced at higher winds and current speeds [22].

Previous studies showed the scarcity of research conducted to investigate the effect of lateral loads on the lateral response of the turbine structure, especially of monopile type, which is the common type in marine wind turbine support applications in shallow areas. As a result, most of the studies and various research methods focused on the issue of the accumulation of the displacement of the structure and its effect on the resistance of the soil over time. Some of the others focused on extracting the forces arising from the aerodynamics in isolation or with the hydrodynamic forces applied based on the turbine support structure, but without going into the calculation of the value of the deflection of the structure and the two forces combined.

The research aims to obtain the characteristics of sea waves through experimental work after fixing five sea wave velocities and then obtaining the values of the lateral forces of the wind and the sea wave affecting the structure of the turbine. This is achieved through a simulation in the ANSYS-Fluent software by extracting the values of the greatest deflection to the structure, then substituting the forces extracted from the simulation into the Euler-Bernoulli bending torque equation to extract the greatest deflection of the structure after integrating the equation twice.

2. Research Methodology

The research will adopt a modern approach based on finding the characteristics of sea waves through experimental work by using a water basin experiment that contains a wave maker and a wind turbine support structure, and a hub with the three turbine blades attached, manufactured by a 3D printer. The experimental model has been scaled down by a scaling factor (1:59.65) with the reliance on Froude's laws in this area. The speed of the five waves was determined based on our assessment of the speed of the Arabian Gulf waves through previous studies and the marine meteorology of the countries of the Arabian Gulf region. The experimental work provided us with the characteristics of each wave in terms of wavelength and height to take advantage of those values after multiplying them by the scaling factor to provide them to the simulation program. To complement the novelty in extracting the deflection values on the theoretical side, the results of the forces of wind loads and sea wave's loads were extracted from the ANSYS-Fluent program instead of extracting the sea wave's load with Morrison's equation to calculate the wave force. The structure was created in real dimensions using SolidWorks to feed the simulation software with the required parameters. Initially, the values of wind forces and wave forces on the structure were calculated by CFD simulation in ANSYS-Fluent software and extracted the maximum deflection value of the structure. Moreover, to increase the simulation results' reliability, we will find the maximum deflection of the structure by theoretically setting the Euler-Bernoulli bending moment equation for the structure and depending on the forces obtained from the simulation to replace it in the mentioned equation.

The idea of the research was based on calculating the values of the dynamic loading forces of the wind and the wave using the ANSYS-Fluent program by using an OWT monopile type [23] with specifications (NREL) rotor that a generating power of (1.5 MW) [24], as shown in Table 1.

Given the difficulty of making a simulation of this size of complexity, due to exposing the entire structure to the forces of wind combined with the forces of the sea wave and in the case of rotating wind turbines, and for the many cases of characteristics sea waves, and to reduce the simulation time, the matter became to make two simulations, the first for five cases of sea wave with constant wind speed for all cases. The turbine blades remain stationary without rotating. The purpose is to identify the condition that may be critical and cause concern about the reliability of the structure. Thus, we will repeat the structure simulation for that case only (the same characteristics of the sea wave and at the same wind speed) but when the turbine blades rotate at 20.5 rpm.

In both simulations, the structure was exposed to severe environmental conditions. Therefore, the solution domain around the offshore wind turbine was divided into two domains to consider the different environmental properties of the wind and the sea wave. In the first simulation, the program was provided with five sea wave characteristics, as shown in Table 2, with a constant wind speed of (12 m/s). In the second simulation, the program was provided with the characteristics of the critical state only, the fifth state, which was inferred from the results of the first simulation, while exposing the structure at the same

time to a constant wind speed of (12 m/s) and the speed of rotation of the turbine blades of (20.5 rpm). The theoretical side was also repeated based on the results of both simulations.

The linear wave theory or (Airy wave theory) is one of the theories that has been used to develop the numerical methods used in the program ANSYS-Fluent. It is one of the most basic theories for describing wave kinematics. Despite its limits due to its simplicity, it is nonetheless applicable to coastal engineering techniques. Among the general assumptions made in developing linear wave theory, the fluid is incompressible. The surface tension can be neglected. A uniform and constant pressure prevail at the free surface, the flow is irrotational, the seabed is horizontal and impermeable, and the wave amplitudes are small compared to the wavelength [25].

Table 1: The specifications of the support structure and the offshore wind turbine [23][24]

Property	Full-Scale	Property	Full-Scale
Rated Rotor Speed	20.5 rpm	Diameter of Tower	4 m
Rated Wind Speed	12 m/s	Diameter of Foundation	3.5 m
Blade Length	34 m	Thickness of Tower	0.05 m
Tower Length	80 m	Thickness of Foundation	0.085 m
Foundation Length (Monopole Length, Monopile Length)	45m (15 m, 30 m)	Material of Tower And Foundation	STEEL
Hub Height	84 m	Average Water Level Above the Seabed	15 m
Rotor Diameter	70 m	Young's Modulus of Tower and Foundation	200 GPa

Table 2: Speed of sea waves [26][27][28][29], and its characteristics from experimental work

Case No.	wave velocity (m/s)	Wave	Case No.
1	0.25	36	1.79
2	0.5	32	2.39
3	0.75	31	2.98
4	1	27	2.39
5	13.88	18	2.98

3. Experimental Work

This section aims to create a scaling model that experimentally simulates a 1.5 MW NREL turbine model carried on a support structure in the form of a hollow cylinder with a diameter of 4 m for the tower and a thickness of 50 mm. A diameter of 3.5 m for the foundation and a thickness of 85 mm [23] to obtain the rest of the characteristics of the sea wave after the wave is thrown with the proposed speed, as well as to compare the results of the amount of deflection in structure through this work with the results of the second simulation program and the results of theoretical equations. Where the wind turbine specifications were obtained from the references [24][30].

The scaled-down model consists of a vertical hollow cylindrical tube. The cylinder height is 159 cm, which simulates the tower's length, plus the length of the submerged foundation and places. It was installed in a water basin.

The three blades of the turbine were made by a 3D printer. The blade length is 57 cm and installed inside the hub, which in turn was installed on a horizontal shaft carried by two bearings placed on a piece of a plate of steel welded to the top of the tower. The hollow cylinder is exposed to waves generated by a wave maker. It moves horizontally through a connecting rod to a disk mounted on a shaft rotated by a motor. It is also exposed to wind forces through a fan installed for this purpose (it projects the winds onto the blades of the turbine and the tower through a specially designed air duct) generated water waves. We assumed that the environment in which the offshore wind turbine structure is located is the marine environmental and climatic conditions of the Arabian Gulf region, where wind data was taken from the website (Global Wind Atlas) [31].

Wind force and water wave force sensors were used on the cylindrical structure. In addition, a digital indicator was used to measure the deflection in the turbine support structure by measuring the horizontal displacement of the top of the tower.

After evaluating and studying the speed of the Arabian Gulf water waves through our available references [32-37].

Table 3 shows the scaling of common parameters for offshore wind turbines' structure and wave characteristics according to Froude's laws. [38,39].

The scaling factors in Table 3 characterize a wind turbine with a monopile support structure and are a function of the scale parameter lambda. It is defined as the ratio of the length scale between the two full-scale and miniature models it dimensions are described in Table 4.

Table 3: Scaling factors for monopile offshore wind turbine structure model testing

Parameter	Scale Factor
Acceleration	1
Force (e.g., wind, wave, structural)	λ_l^3
Stress	λ_l
Area Moment of Inertia	λ_l^4
Length (e.g., displacement, wave height)	λ_l
Area	λ_l^2
Density	1
Mass	λ_l^3
Time (e.g., wave period)	$\lambda_l^{0.5}$
Frequency (e.g., rotor rotational speed)	$\lambda_l^{-0.5}$
Velocity (e.g., wind speed, wave celerity)	$\lambda_l^{0.5}$

Table 4: Real and experimental model specifications for the NREL-1.5 MW Offshore Wind Turbine and support structure With scaling parameter λ_l = 1:59.65

Property	Real	Model
Rated Wind Speed	12 m/s	1.55 m/s
Blade Length	34 m	57 cm
Tower Length	80 m	134 cm
Monopole Length	15 m	25 cm
Hub Height	84 m	140.8 cm
Rotor Diameter	70 m	117 cm
Diameter of Tower	4 m	6.7 cm
Diameter of Foundation	3.5 m	5.9 cm
Thickness of Tower	0.05 m	0.84 mm
Thickness of Foundation	0.085 m	1.43 mm
Material of Tower and Pile	STEEL	STEEL
Average Water Level Above the Bottom	15 m	25 cm
Young's Modulus of Tower and Pile	200 GPa	200 GPa

3.1 Experiment Equipment

A rectangular water basin was made by welding four iron pieces, three of which were circumferential, the fourth had a base, and the front side near the researcher was made of glass. The turbine support structure (The hollow cylinder representing the tower and part of the foundation, which is the part immersed in water) is installed in the middle of the water trough. It has a wave absorber at the end to ensure the wave does not bounce. Figure 2 shows the details and components of the water basin. The work of the experiment required us to make waves at different speeds (five speeds were determined), the first four speeds simulated normal sea conditions and the fifth speed simulated the state of turbulence in seawater. Wavemaker manufactured an electromechanical system by vertical plate, depending on the reference[40]. To increase the efficiency of the test and to pass one of the experimental work problems related to the flow, which is the wave recoil from the far end of the source, we worked on making a wave absorber. An electric air fan is installed on a base that is not connected to the water basin, and it pushes the air towards the blades and the tower on one horizontal axis. To obtain data on the forces that the wind or waves exert on the structure, a load cell sensor of the type ROHS-10KG was used. Usually, the signal output of the electrical power from the load cell is very small. Therefore, it needs a signal amplifier, so an HX711 load cell signal amplifier was used to connect through the four wires to the Arduino. Digital Indicator is measuring instruments that ensure high quality. Our practical study used it to measure the maximum deflection that can occur at the maximum point in the tower. It accurately measures small linear distances in mechanical and industrial processes without reading errors.

Figure 2: Experiment equipment

4. Structure Simulations by ANSYS-Fluent R19

4.1 Model Design

Designing the model requires real dimensions obtained from standard sources, as the shape and dimensions of the blade edges represent the main part of the construction and design of the model, as shown in Figure 3. That the model's design is not the final design for a simulation in ANSYS-Fluent, because it is just a stereotype, devoid of additions or boundaries in which the liquid is formed in relation to the waves. We note from Figure 3 that the model was divided into two domains. The first domain, the small one, is movable and contains the turbine blades and hub. The second domain, which is large, contains the tower and other parts to calculate the forces extracted from the simulation program. The turbine blade area is exposed to the wind at a speed of 12 m/s and rotates at a rotational speed of (20.5 rpm). The tower area is exposed to the wind at the same speed. And the foundation area was exposed to the forces of sea waves at a speed wave of 13.88 m/s.

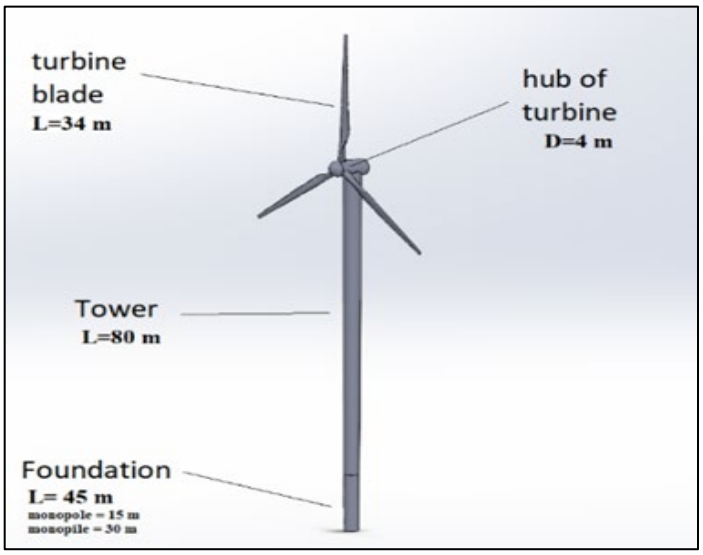

Figure 3: The geometry of the model under study

4.2 Domains, Initial Boundary Conditions, and Meshing

To obtain accurate results through the simulation program, we make a mesh for the model, where this mesh works to solve the complex equations to get the results. For an integrated mesh to be made accurately and correctly, the stereogram must be organized in a manner commensurate with the construction of the mesh, where the model was completely divided into two sections. The first section represents the large model (big domain), which has a mesh related to sea waves and wind flow, and then the small model (small domain) that surrounds the turbine blades to increase the mesh of blades and work to calculate the forces accurately, where the dimensions were used as shown in the Figure (4).

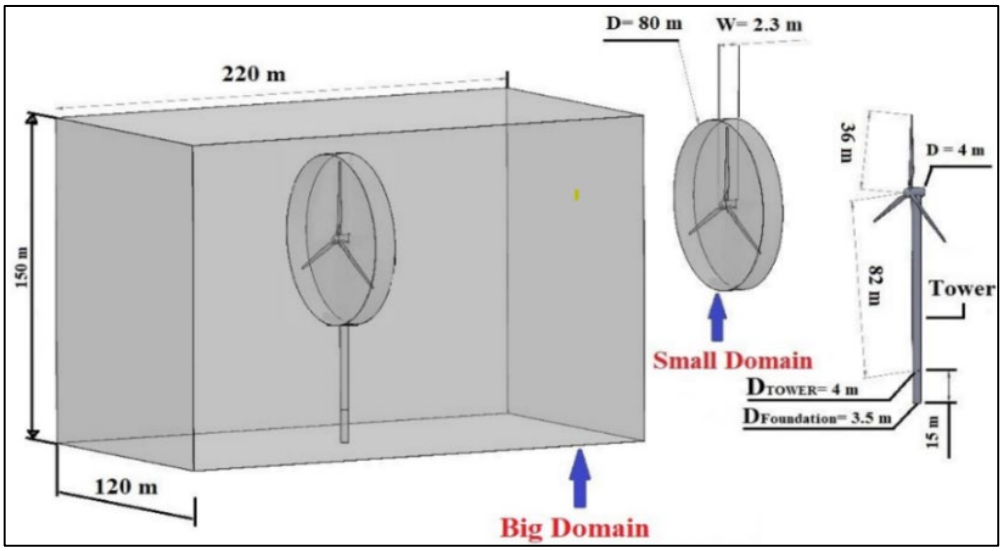

Figure 4: Dimension of domain parts

After completing the design process completely in the Solid Works program, it was exported in the Para solid format to be received in the simulation program.

Simulation software settings are the basic upon which complex equations are based. For example, the standard k-epsilon model [41], was used for the velocity model because it is very accurate in these processes. On the other hand, the VOF model [41], was used for the multi-stage model to define wind and water, as shown in Table 1.

The first step of the simulation process after importing the stereo file is the mesh stage to obtain accurate results in the simulation, as shown in Figure 5. The gradual development of the mesh reached the number of nodes (404247) and the number of elements (2185917), where the type of mesh in the ANSYS-Fluent program was (Tetrahedral Elements).

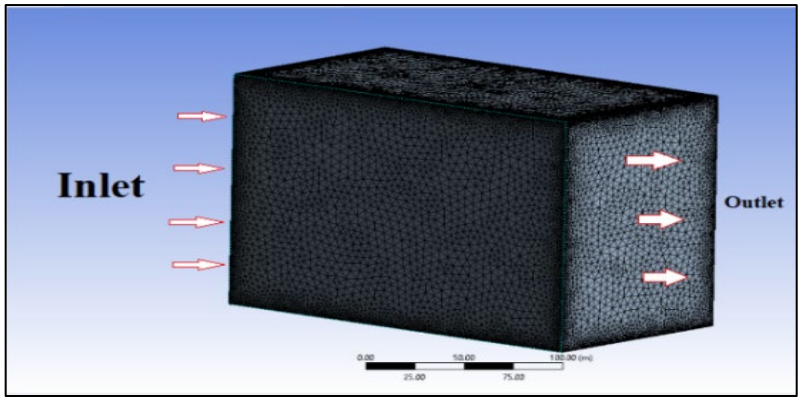

Figure 5: Mesh of small and big domain

After completing the settings of the CFD program, it is linked with the structural program (Structural analysis is one of the most widely used areas of application of finite element analysis methods). The structure that can be completed by ANSYS Analysis includes static structural analysis, nonlinear structural analysis, Structural dynamics analysis), Static structure analysis is a basic procedure for designing the structure using which the structure's response to applied external forces can be obtained ،It also assesses whether the specific structural design will withstand external and internal stresses and forces. Through it, we can determine the behavior of the material model. Structural dynamics analysis studies the structure's response to dynamic loads (such as the chronological history of displacement, stress, acceleration, etc.). Figure (6) shows the direction of the forces resulting from the wind and the sea waves and the coordinates through which the work plane is located in the program. (Y) is positive towards the top of the structure, and (Z) positive is the direction of wind movement and the movement of sea waves on the structure. Weights are added to the tower and the area of the turbine blades as well as an installation area on the foundation to see the distortions and stresses that get it. The rotation of the moving part of the structure (wind turbine blades) with a speed of (20.5 rpm), the time of each step was set by (0.1 s) for the number of steps of 100. The implementation time of the program took 4 hours, as shown in Figure 7.

5. Theoretical Calculation

The structure will be likened to a cantilever beam is simply defined as a beam with one fixed end and the other as a free end, as shown in Figure 8. We anticipated that any shear deformations would be minor. Therefore, we only looked at deflection caused by pure bending. Although there are basically many important methods by which we can easily determine the deflection at any section of a loaded structure, in our research, we will use the double integration method.

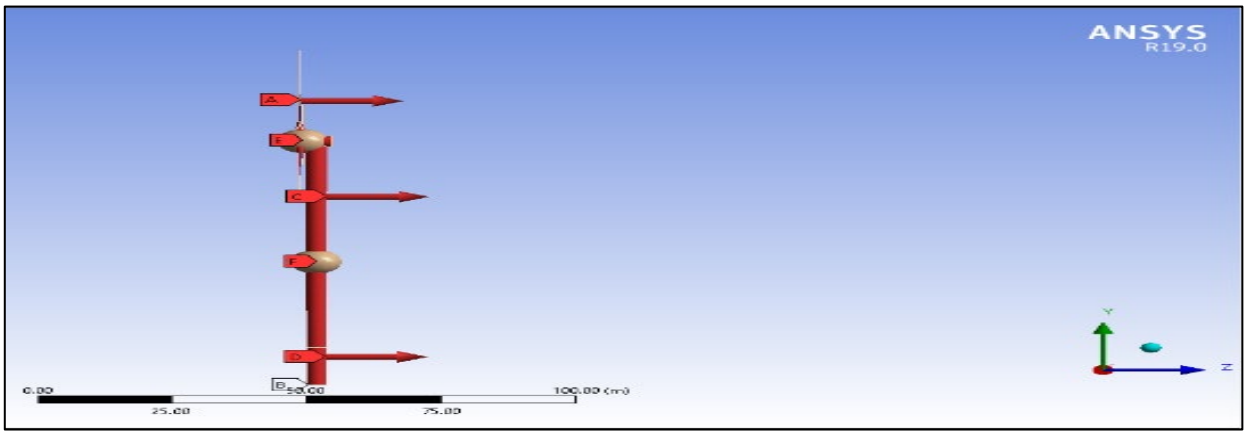

Figure 6: The direction of the forces that the structure is subjected

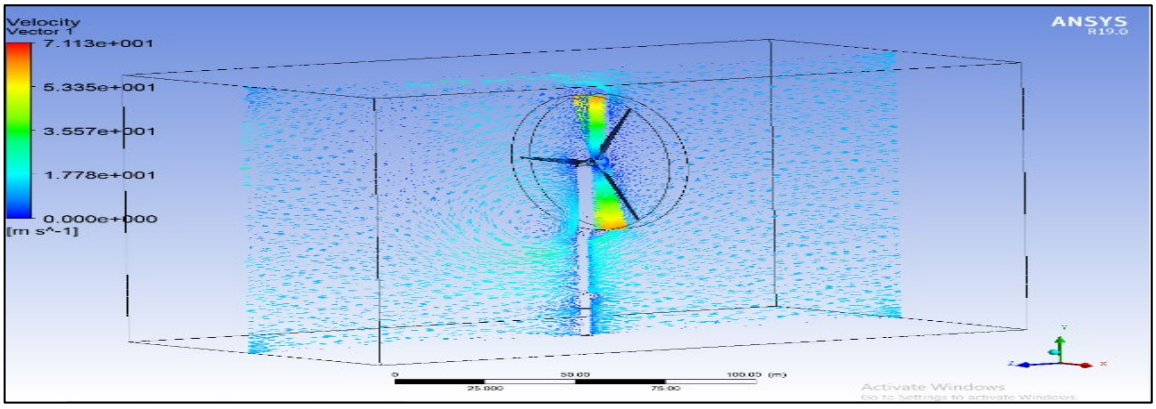

Figure 7: Wind movement at 12 m/s and water wave movement at 13.88 m/s over the entire structure of the model

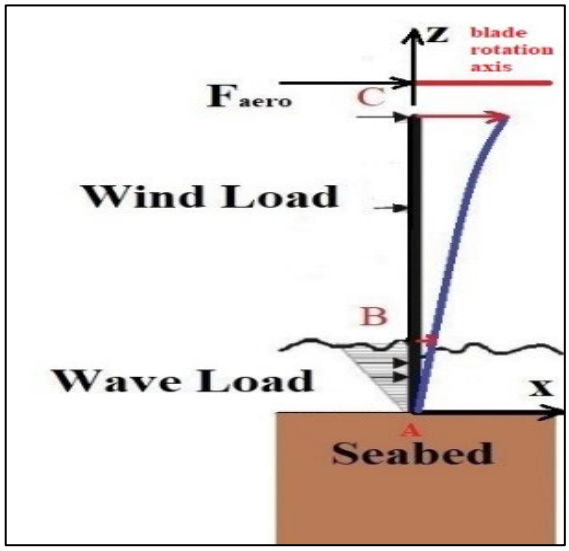

Figure 8: A cantilever monopile structure

To find the deflection and slope, we do the following:
The equivalent moment of inertia was calculated for the whole structure.

The wind force combined with the wave force of the water was calculated based on the ANSYS-Fluent program. Using the program, we calculated three forces that affect the structure.

The first force, its symbol (F_{aero}) represents the average wind force on the wind turbine blades. The position of its focus is chosen on the axis of rotation of the turbine blades, horizontally and in the positive x direction. The second force is the average wind force on the tower and is denoted by (F_{WIND}), its focus is located horizontally in the middle of the tower area. The third power is the average wave power of the water on the foundation of the supporting structure and is indicated with a sign (F_{wave}) and its center is located horizontally in the middle of the length of the foundation.

We will derive the bending moment equation for the structure and solve it by the double integration method as follows:

We will draw a free-body diagram showing where the forces affect the structure and mark two parts that cut the structure. The first G-G cuts the structure at the bottom of the tower and before the foundation area. The second S-S cuts the structure in the area below the foundation, as shown in Figure 9.

EI_{tower}= 242.06 ×10^9 N.m^2, $EI_{found.}$ = 266.052 ×10^9 N.m^2.

$$\sum M = 0 \qquad The\ direction\ of\ the\ positive\ moment\ is\ clockwise$$

Segment BC: $0 \leq Z \leq 82$

$$[M(z) + F_{aero} \cdot Z + F_{WIND} \cdot (Z - 42)] = 0 \tag{1}$$

$$EI\frac{d^2x}{dz^2} = M(z)_{G-G} = -[F_{aero} \cdot Z + F_{WIND} \cdot (Z - 42)] \tag{2}$$

Integrating 1

$$\frac{dx}{dz} = \theta_{BC} = \frac{1}{EI_{tower}}\left[-\left[F_{aero} \cdot \frac{Z^2}{2} + F_{WIND} \cdot \frac{(Z-42)^2}{2}\right] + C1\right] \quad (3)$$

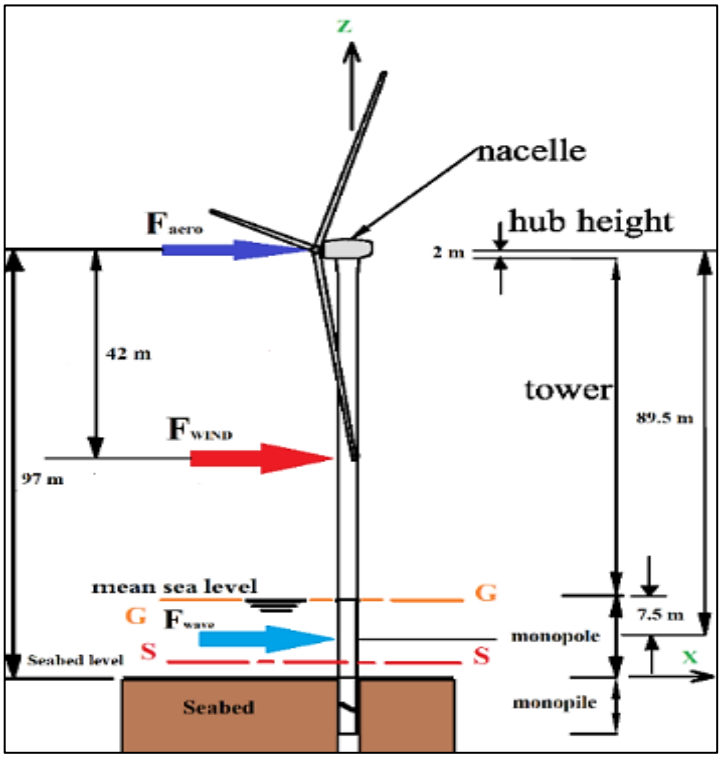

Figure 9: Free body diagram of the structure

Integrating 2

$$X_{BC} = \frac{1}{EI_{tower}}\left[-\left[F_{aero} \cdot \frac{Z^3}{6} + F_{WIND} \cdot \frac{(Z-42)^3}{6}\right] + C1 \cdot Z + C2\right] \quad (4)$$

Segment AB: $82 \leq Z \leq 97$

$$EI\frac{d^2x}{dz^2} = M(z)_{S-S} = -\begin{bmatrix} F_{aero} \cdot Z + F_{WIND} \cdot (Z-42) + \\ F_{wave} \cdot (Z-89.5) \end{bmatrix} \quad (5)$$

First integration:

$$\frac{dx}{dz} = \theta_{AB} = \frac{1}{EI_{found.}}\left[-\begin{bmatrix} F_{aero} \cdot \frac{Z^2}{2} + F_{WIND} \cdot \frac{(Z-42)^2}{2} + \\ F_{wave} \cdot \frac{(Z-89.5)^2}{2} \end{bmatrix} + C3\right] \quad (6)$$

Second integration:

$$X_{AB} = \frac{1}{EI_{found.}}\left[-\begin{bmatrix} F_{aero} \cdot \frac{Z^3}{6} + F_{WIND} \cdot \frac{(Z-42)^3}{6} + \\ F_{wave} \cdot \frac{(Z-89.5)^3}{6} \end{bmatrix} + C3 \cdot Z + C4\right] \quad (7)$$

Boundary condition for fixed support at point A: When Z=97; the slope (θ) = 0, the deflection (X) = 0.Use eq. (6):

$$EI\frac{dx}{dz} = EI\theta = 0 = -\begin{bmatrix} F_{aero} \cdot \frac{(97)^2}{2} + F_{WIND} \cdot \frac{(97-42)^2}{2} + \\ F_{wave} \cdot \frac{(97-89.5)^2}{2} \end{bmatrix} + C3 \quad (8)$$

We will get:

$$C3 = \begin{bmatrix} F_{aero} \cdot \frac{(97)^2}{2} + F_{WIND} \cdot \frac{(97-42)^2}{2} + \\ F_{wave} \cdot \frac{(97-89.5)^2}{2} \end{bmatrix} \quad (9)$$

If we use Eq. (7):

$$X_{AB} = 0 = -\begin{bmatrix} F_{aero} \cdot \frac{(97)^3}{6} + F_{WIND} \cdot \frac{(97-42)^3}{6} + \\ F_{wave} \cdot \frac{(97-89.5)^3}{6} \end{bmatrix} + C3 \cdot 97 + C4 \quad (10)$$

We will get:

$$C4 = \begin{bmatrix} F_{aero} \cdot \frac{(97)^3}{6} + F_{WIND} \cdot \frac{(97-42)^3}{6} + \\ F_{wave} \cdot \frac{(97-89.5)^3}{6} \end{bmatrix} - C3 \cdot 97 \quad (11)$$

At point B, the slope and deflection are the same at the top and bottom of the point.
At point B: when Z = 82 m, use Eq. (3) and (6)
Top: $0 \leq Z \leq 82$
Bottom: $82 \leq Z \leq 97$

$$\frac{1}{EI_{tower}}\left[-\left[F_{aero} \cdot \frac{(82)^2}{2} + F_{WIND} \cdot \frac{(82-42)^2}{2}\right] + C1\right]$$
$$= \frac{1}{EI_{found.}}\left[-\begin{bmatrix} F_{aero} \cdot \frac{(82)^2}{2} + F_{WIND} \cdot \frac{(82-42)^2}{2} + \\ F_{wave} \cdot \frac{(82-89.5)^2}{2} \end{bmatrix} + C3\right] \quad (12)$$

We will get:

$$C1 = \begin{bmatrix} \frac{1}{EI_{found.}}\left[-\begin{bmatrix} F_{aero} \cdot \frac{(82)^2}{2} + F_{WIND} \cdot \frac{(82-42)^2}{2} + \\ F_{wave} \cdot \frac{(82-89.5)^2}{2} \end{bmatrix} + C3\right] \\ + \frac{1}{EI_{tower}}\left[F_{aero} \cdot \frac{(82)^2}{2} + F_{WIND} \cdot \frac{(82-42)^2}{2}\right] \end{bmatrix} \cdot EI_{tower} \quad (13)$$

At point B: when Z = 82 m, use eq. (4) and (7)
Top: $0 \leq Z \leq 82$
Bottom: $82 \leq Z \leq 97$

$$\frac{1}{EI_{tower}}\left[-\left[F_{aero} \cdot \frac{(82)^3}{6} + F_{WIND} \cdot \frac{(82-42)^3}{6}\right] + C1 \cdot 82 + C2\right]$$
$$= \frac{1}{EI_{found.}}\left[-\begin{bmatrix} F_{aero} \cdot \frac{(82)^3}{6} + F_{WIND} \cdot \frac{(82-42)^3}{6} + \\ F_{wave} \cdot \frac{(82-89.5)^3}{6} \end{bmatrix} + C3 \cdot 82 + C4\right] \quad (14)$$

We will get:

$$C2 = \frac{1}{EI_{tower}}\left[\left[F_{aero}\cdot\frac{(82)^3}{6} + F_{WIND}\cdot\frac{(82-42)^3}{6}\right] - C1\cdot 82\right] + \frac{1}{EI_{found.}}\left[-\left[\begin{matrix}F_{aero}\cdot\frac{(82)^3}{6} + F_{WIND}\cdot\frac{(82-42)^3}{6} + \\ F_{wave}\cdot\frac{(82-89.5)^3}{6}\end{matrix}\right] + C3\cdot 82 + C4\right]\cdot EI_{tower} \quad (15)$$

Then we substitute the integration constants (C1=547178517.11, C2=-42701262505.2, C3=643078523.5, and C4=-50059661828.79) in equations (3, 4, 6, and 7), respectively to get general equations for slope and deflection for the entire structure. Therefore, if we substitute the value of (Z) = 0 at point C, we will get the maximum slope and deflection at the top of the structure.

$$\theta_C = \frac{1}{EI_{tower}}\left[-\left[F_{aero}\cdot(0) + F_{WIND}\cdot\frac{(0-42)^2}{2} + \right] + C1\right] \quad (16)$$

$$X_C = \frac{1}{EI_{tower}}\left[-\left[F_{aero}\cdot(0) + F_{WIND}\cdot\frac{(0-42)^3}{6} + \right] + C1\cdot(0) + C2\right] \quad (17)$$

6. Results and Discussion

6.1 Experimental Work Results

Figure 10 shows the graphs of the distribution of wind forces and wave forces on the structure for five cases of water wave velocity after 20 seconds from the start of the test by reading the force sensors distributed on the structure associated with the Arduino program.

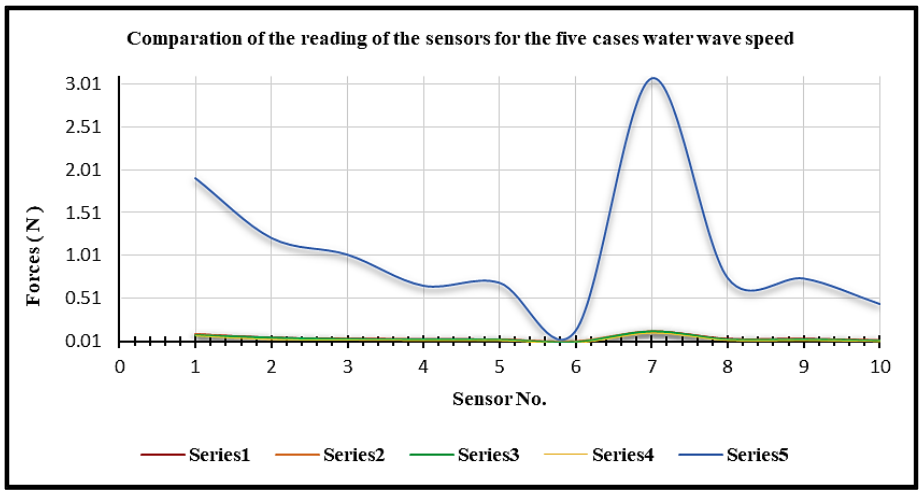

Figure 10: Comparison of the ten sensor readings for the five cases combined

Show that the distribution of wind forces and wave forces on the structure were distributed in the form of a regular triangle. Its base is at the top for each wind and wave force.

Table 5 shows the most important characteristics of scaled water waves based on sea wave data in the Arabian Gulf region and wave criteria.

The device (digital indicator) reads the values of the horizontal displacement of the top of the tower in the direction of the wind flow and the wave flow for five different wave velocity cases while keeping the wind speed applied to the structure constant at 1.55 m/s for the five cases. Table 6 shows the results we have reached.

Table 5: Shows characteristics of scaled water waves in water basin and wave's criteria

Case No.	Wave velocity (m/s)	Wave height, H (cm)	Wavelength ,λ (cm)	$\frac{h = 25cm}{\lambda}$	$\frac{H}{\lambda}$	$\frac{D_{pile} = 5.9cm}{\lambda}$
1	0.032	2	84	0.297	0.024	0.07
2	0.065	3	75	0.333	0.04	0.079
3	0.097	4	70	0.357	0.057	0.084
4	0.129	3	66.5	0.376	0.045	0.089
5	1.799	4	55	0.455	0.073	0.107

Table 6: Shows the values of the greatest deflection that occur for the scaled structure

Case No.	Maximum deflection (mm)
1	0.55
2	0.60
3	0.58
4	0.6
5	3.00

The results of the digital indicator for measuring the horizontal displacement shown in Table 6 show the convergence of the deflection values in the structure for the first four cases and the increase in its value in the fifth case, where it reached such (3 mm). The results also show a decrease in the deflection value of the structure in the third case, despite the similarity of the wave height with the fifth case. Still, the difference was in the wave velocity for both cases, which leads to the belief that the speed of the water wave has a greater impact on the structure than its height. The value of the structure deflection for the fifth case is equal to (0.178 m) after being multiplied by the scaling factor's value (1:59.65).

6.2 Simulation ANSYS-Fluent Results

The results of the first simulation (steady state) shown in Table 7 showed that the fifth case of the sea wave cases is the critical case, so a second simulation (unsteady state) of the structure was carried out with the program providing the characteristics of this case only. In conjunction with the structure's exposure to a constant wind speed as in the first simulation. the results of the second simulation came with new and significant values of forces greater than the values in the first simulation, as shown in Figure 11 and Table 8. The results showed that the rotation of the turbine blades plays a major role in adding greater stresses than if the turbine was not working, and with the large increase in the result of the deflection of the structure from the first simulation, which was valued (0.15 m), but still the value of the maximum deflection of the structure (0.2016 m), which came with the second simulation did not reach the maximum permissible deflection whose value is (0.338 m).

Table 7: The forces values result of the first simulation (steady state)

Case No.	Wave speed(m/s)	Wavelength (m)	Location	Force (N)
1	0.25	36	Blades rotation axis (Hub)	24432.309
			Middle of the Tower	4688.7
			Middle of the Foundation	53295.996
2	0.5	32	Blades rotation axis (Hub)	24732.004
			Middle of the Tower	5638.3
			Middle of the Foundation	37379.469
3	0.75	31	Blades rotation axis (Hub)	24205.496
			Middle of the Tower	3316.1
			Middle of the Foundation	68405.445
4	1	27	Blades rotation axis (Hub)	24809.381
			Middle of the Tower	5232.5
			Middle of the Foundation	62946.914
5	13.88	18	Blades rotation axis (Hub)	21525.977
			Middle of the Tower	208336.6
			Middle of the Foundation	2277959.5

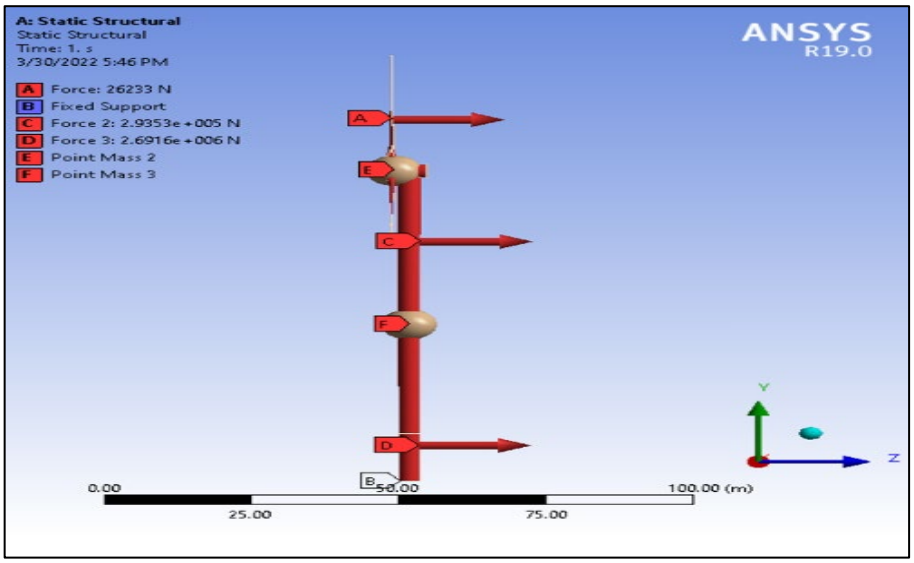

Figure 11: The forces values on the structure

Table 8: The effect of force on structure and forces value in the second simulation (unsteady state)

Case No.	Wave speed (m/s)	Wavelength (m)	Location	Force (N)
1	13.88	18	Blades rotation axis (Hub)	26233
			Middle of the Tower	293530
			Middle of the Foundation	2691600

Naturally, the large value of the sea wave force in the foundation area will increase the stresses in that area to reach its value within (4.07e7 Pa) at the end of fixing the structure with the seabed, as shown in Figure 12.

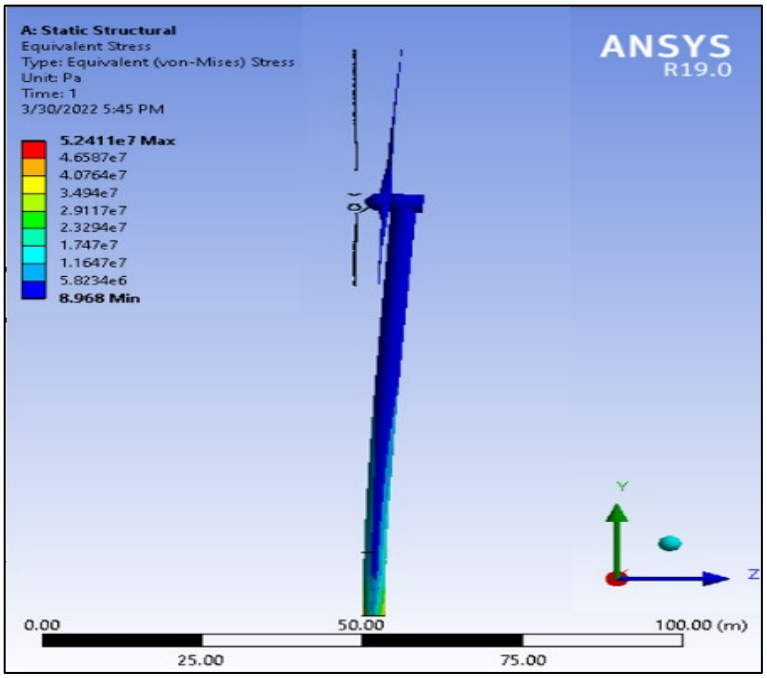

Figure 12: Stress values of an offshore wind turbine structure in the second simulation

The forces of sea waves with wind forces on the structure lead to an increase in the deflection of the structure in the positive direction of those effects. Figure 13 shows that the greatest deflection occurs to the structure at the top in the (hub), where its value is (0.201m).

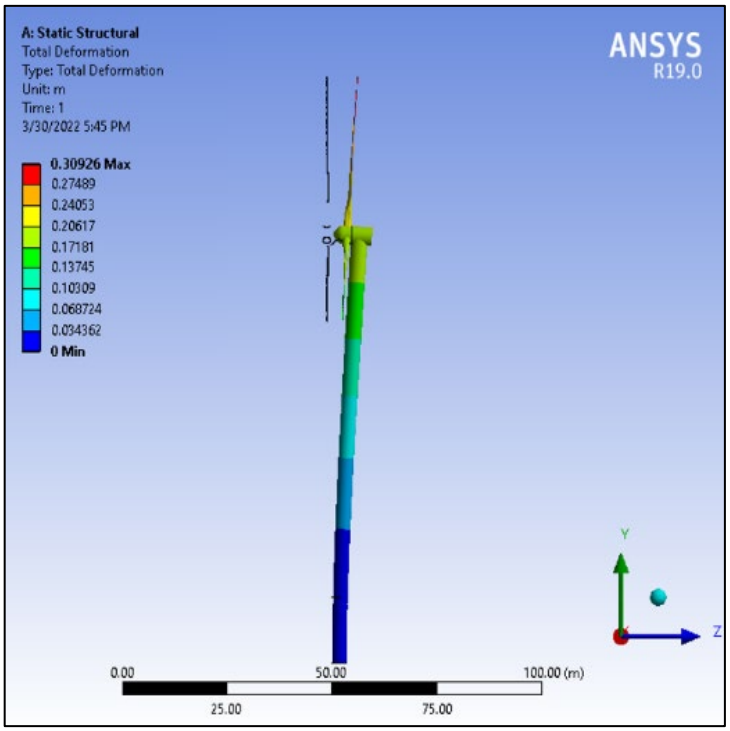

Figure 13: Offshore wind turbine deflection

The result of the safety factor of the structure came in favor of the reliability of the structure, as shown in Figure 14. The results show that the safety factor for most parts of the structure is about (15), except for the lower part of the foundation, which is about (10).

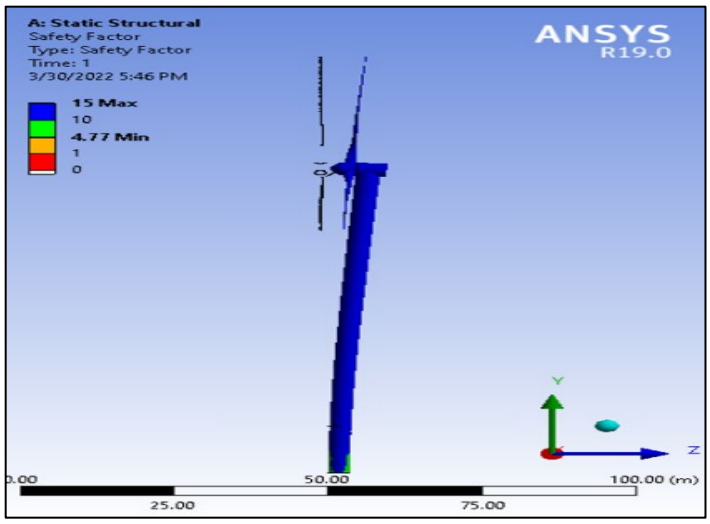

Figure 14: Offshore wind turbine safety factor

6.3 Theoretical Results

Substituting the results of the forces extracted from the first simulation and given in Table 7 into the equations of the theoretical side, the results are the maximum deflection value of the structure (0.108m) and the slope value (0.037 degrees) in the fifth case, where the values of the stresses on the structure were as in Figure 12.

Substituting the results of the forces extracted from the second simulation and given in Table 9 into the equations of the theoretical side, the results are the maximum deflection value of the structure (0.160 m) and the slope value (0.068 degrees).

The results showed us, as in Figure 15, that the values of the structure deflection resulting from the simulation work in the ANSYS-Fluent software were higher than in the theoretical work. But the results in both cases are within the permissible limits for deflection of the structure with such dimensions. The maximum permissible deflection is (0.338 m). Thus, the support structure under study is considered successful in this aspect.

Table 9: Maximum bending stress in the first simulation

Case No.	Maximum bending stress KN/m^2
1	19.751
2	19.419
3	20.035
4	20.665
5	78.299

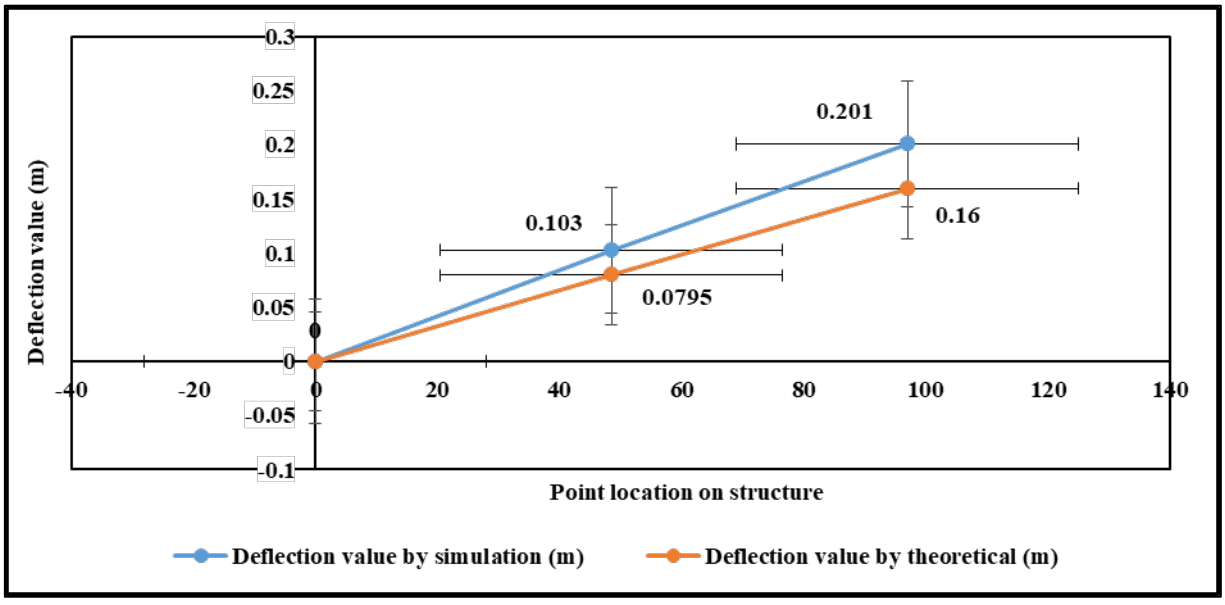

Figure 15: A comparison between the results of the second simulation work and theoretical work

7. Conclusion

The study's objectives included knowing the values of the deflection and slope of the support structure of an offshore wind turbine as a result of being affected by the dynamic wind loads combined with the dynamic loads of sea waves. The desired aims were reached in several ways, including theoretical calculations and readings of the experimental work, as well as a full-scale simulation in the ANSYS-Fluent program. From all of the above, we came up with several conclusions, including:

1) The rest of the characteristics of the sea wave were extracted through experimental work after fixing the velocity of the sea wave in light of the 1- The rest of the characteristics of the sea wave were extracted through experimental work after determining the speed of the sea wave in light of the values of the water wave speed of the Arabian Gulf in the previous research references for use in the simulation program. The results showed the convergence of the wave height values for the last four cases, which ranged from 3 cm to 4 cm, despite the difference in wavelengths for all cases, especially the fifth case, which had a wavelength of 55 cm, and wave speed of 1.799 m/s.
2) The simulation (CFD) was conducted twice to extract the forces acting as a result of the lateral loads of wind and sea waves on the structure and obtain the deflection values. The values of the deflection of the first simulation are close and small, except for the value of the fifth case, which was higher. This is due to the increase in the wave force in this case. The value of the deflection of the structure reached (0.15 m). In contrast, the deflection value at the top of the structure in the second simulation of the same case, but with the rotation of the turbine blades of (0.201 m). This is a result of the effect of the increased strength resulting from aerodynamics on the structure. On the other hand, increasing the result of the largest deflection value of the structure for the second simulation for the fifth case came with a noticeable increase in the values of stresses applied to the structure. This is due to the rotation of the turbine blades. It also affected the increase in the result of the structural deflection values in the theoretical calculations, whose value, depending on the forces obtained from the second simulation, reached (0.16 m), while its value was, depending on the forces obtained from the first simulation (0.108 m).
3) The results showed that wave characteristics (speed, height, wavelength, and others) play a major role in increasing or decreasing water wave loads, especially wave speed and wavelength. In addition, the results showed that the forces generated by the turbine blades' rotation greatly increased the lateral stresses on the structure.
4) The results of the deflection of the structure were within the permissible limit of the deflection, which is (0.338 m). The results are consistent with what is common in multi-methodological studies, i.e., that the simulation results are more valuable than the results of the experimental work and the theoretical approach.
5) The result of the structure's safety factor showed the structure's reliability when exposed to wind loads and sea waves at high speed, reaching 15 in most of the structure, while in the lower foundation area, it reached 10.
6) Figure 15 shows the difference between the results of the work of the second simulation and the theoretical equations based on the forces obtained from the second simulation. The difference in the results of the two approaches stems from the different calculation methods. In the simulation, the program does not stop until the number of iteration steps is set at the beginning of the program installation. Then, the value of the difference between each iteration is determined. When the pre-set value is reached, the program is stopped. Whereas in theoretical mathematical equations, boundary conditions predominate in calculating the constants of integration.

Author contribution

All authors contributed equally to this work.

Funding

This research received no specific grant from any funding agency in the public, commercial, or not-for-profit sectors.

Data availability statement

The data that support the findings of this study are available on request from the corresponding author.

Conflicts of interest

The authors declare that there is no conflict of interest.

References

[1] J. van der Tempel, N. F. B. Diepeveen, D. J. C. Salzmann, W. E. de Vries, Design of support structures for offshore wind turbines, in Wind Power Generation and Wind Turbine Design, WIT Trans. State Art Sci. Eng., 44 (2010) 559–591. https://doi.org/10.2495/978-1-84564-205-1/17

[2] S. Sánchez, J. S. López-Gutiérrez, V. Negro, M. D. Esteban, Foundations in offshore wind farms: Evolution, characteristics and range of use. Analysis of main dimensional parameters in monopile foundations, J. Mar. Sci. Eng., 7 (2019). https://doi.org/10.3390/JMSE7120441

[3] J. Klijnstra, X. Zhang, S. van der Putten, and C. Röckmann, Technical Risks of Offshore Structures, 2017.

[4] J. H. Ferziger, M. Perić, R. L. Street, Computational Methods for Fluid Dynamics, Fourth Edi. Springer, 2020.

[5] D. Chen, K. Huang, V. Bretel, L. Hou, Comparison of Structural Properties between Monopile and Tripod Offshore Wind-Turbine Support Structures, Adv. Mech. Eng., 5 (2013) 9. https://doi.org/10.1155/2013/175684

[6] K. Wei, S. R. Arwade, A. T. Myers, Incremental wind-wave analysis of the structural capacity of offshore wind turbine support structures under extreme loading, Eng. Struct., 79 (2014) 58–69, 2014. https://doi.org/10.1016/j.engstruct.2014.08.010

[7] D. Kallehave, B. W. Byrne, C. LeBlanc Thilsted, K. K. Mikkelsen, Optimization of monopiles for offshore wind turbines, Philos. Trans. R. Soc. A Math. Phys. Eng. Sci., 373 (2015).https://doi.org/10.1098/rsta.2014.0100

[8] K. Wei, S. R. Arwade, A. T. Myers, V. Valamanesh, Directional effects on the reliability of non-axisymmetric support structures for offshore wind turbines under extreme wind and wave loadings, Eng. Struct., 106 (2015) 68–79. https://doi.org/10.1016/j.engstruct.2015.10.016

[9] I. Alesbe, M. Abdel-Maksoud, S. Aljabair, Investigation of the Unsteady Flow Behaviour on a Wind Turbine Using a BEM and a RANSE Method, J. Renew. Energy, 2016 (2016) 1–12.https://doi.org/10.1155/2016/6059741

[10] A. K. Samal ,T. E. Rao, Analysis of Stress and Deflection of Cantilever Beam and its Validation Using ANSYS. Int. J. Eng. Res. Appl., 6 (2016) 119–126.

[11] M. Arshad and B. C. O'Kelly, Analysis and Design of Monopile Foundations for Offshore Wind-Turbine Structures, Mar. Georesour. Geotechnol., 34 (2016) 503–525. https://doi.org/10.1080/1064119X.2015.1033070

[12] Turgut "Sarp" Sarpkaya, WAVE FORCES ON OFFSHORE STRUCTURES. Cambridge University Press, 2010.

[13] T. Sarpkaya, In-line and transverse forces on smooth and rough cylinders in oscillatory flow at high Reynolds numbers, Monterey, California, 1986.

[14] P. Dymarski, E. Ciba, T. Marcinkowski, Effective method for determining environmental loads on supporting structures for offshore wind turbines, Polish Marit. Res., 23 (2016) 52–60. https://doi.org/10.1515/pomr-2016-0008

[15] S. Lokesh Ram and R. Mohana, Simulation and numerical analysis of offshore wind turbine with monopile foundation, IOP Conf. Ser. Mater. Sci. Eng., 872, 2020,012046.https://doi.org/10.1088/1757-899X/872/1/012046

[16] H. Alwan, I. Al-Esbe, and S. J. Kadhim., Investigation of Wave Forces on Fixed Monopile Foundation of Offshore Wind Turbine, J. Univ. Babylon Eng. Sci., 28 (2020) 127–143.

[17] S. J. Kadhim, Investigation the environmental conditions on hydrodynamic analysis of two offshore wind turbine foundation, 2020.

[18] Z. Wang, R. Hu, H. Leng, H. Liu, Y. Bai, W. Lu, Deformation analysis of large diameter monopiles of offshore wind turbines under scour, Appl. Sci., (Switzerland), 10 (2020) 1–18. https://doi.org/10.3390/app10217579

[19] J. Zhang, H. Lu, K. Sun, Dynamic response analysis for offshore structures by a combination of segmented responses based on pole-residue method, Ocean Eng., 219 (2021) 108277. https://doi.org/10.1016/j.oceaneng.2020.108277

[20] MALLIKARJUN, C. R, D. S. H. A, B. K. C, P. K, Design and Structural Analysis of Wind Turbine Tower, Int. Res. J. Eng. Technol., 08 (2021) 1284–1301

[21] Z. Gao et al., A brief discussion on offshore wind turbine hydrodynamics problem, J. Hydrodyn., 34 (2022) 15–30. https://doi.org/10.1007/s42241-022-0002-y

[22] A. Buljac, H. Kozmar, W. Yang, A. Kareem, Concurrent wind, wave and current loads on a monopile-supported offshore wind turbine, Eng. Struct., 255 (2022). https://doi.org/10.1016/j.engstruct.2022.113950

[23] A. Kumar, B. Ganesh, D. Ramesh, dynamic analysis of the supporting tower for an offshore wind turbine under wind load, 2015.

[24] J. Rinker and K. Dykes, WindPACT Reference Wind Turbines, Nrel/Tp-5000-67667, no. April, 2018.

[25] D. Markus, A Code Based Methodology to Account for Wave Loading in the Design of Offshore Structures, no. September, 2009.

[26] M. Shaker, Encyclopedia of the history of the Arabian Gulf. Amman - Jordan: Dar Osama for Publishing and Distribution, 2005.

[27] J. K¨ampf ,M. Sadrinasab, The circulation of the Persian Gulf: a numerical study, Ocean Sci. Discuss., 2 (2005) 129–164. https://doi.org/10.5194/os-2-27-2006

[28] Wind & weather statistics Persian Gulf Airport - Windfinder.

[29] The Encyclopedia Americana International, New York: Americana Corporation, 1976.

[30] D. J. Malcolm ,A. C. Hansen, WindPACT Turbine Rotor Design Study: June 2000--June 2002 (Revised), no. April, 2006. https://doi.org/10.2172/15000964

[31] DTU Wind Energy and World Bank Group, Global Wind Atlas, Global Wind Atlas. 28782, 2018.

[32] W. P. Goharnejad, Hamid, Ehsan Nikaien, Assessment of wave energy in the Persian Gulf: An evaluation of the impacts of climate change, Oceanol., 63, 2021. https://doi.org/10.1016/j.oceano.2020.09.004

[33] M. Sharifinia, M. Daliri, E. Kamrani, Estuaries and Coastal Zones in the Northern Persian Gulf (Iran), Coasts and Estuaries: The Future. 2019.https://doi.org/10.1016/B978-0-12-814003-1.00004-6

[34] M. B. A. Milad Rashidinasab, Modeling the Pressure Distribution and the Changes of Water Level around the Offshore Platforms Exposed to Waves, Using the Numerical Model of Flow 3D, Comput. Water, Energy, Environ. Eng., 6 (2017) 97–106.https://doi.org/10.4236/cweee.2017.61008

[35] S. Neelamani, K. Al-Salem, and K. Rakha, EXTREME WAVES FOR DIFFERENT RETURN PERIODS IN THE ARABIAN GULF, 2007.

[36] A. Etemad-Shahidi, B. Kamranzad, V. Chegini, Wave Energy Estimation in the Persian Gulf, 2011.

[37] Y.-P. LIAO and J. M. KAIHATU, Numerical Investigation of Wind Waves in the Persian Gulf: Bathymetry Effects, 2016.

[38] S. Bhattacharya, D. Lombardi, D. M. Wood, Similitude relationships for physical modelling of monopile-supported offshore wind turbines, Int. J. Phys. Model. Geotech., 11 (2011) 58–68.https://doi.org/10.1680/ijpmg.2011.11.2.58

[39] D. Lombardi, S. Bhattacharya, and D. Muir Wood, Dynamic soil-structure interaction of monopile supported wind turbines in cohesive soil, Soil Dyn. Earthq. Eng., 49 (2013) 165–180. https://doi.org/10.1016/j.soildyn.2013.01.015

[40] Q. Chen, X. Chen, Y. Ma, G. Dong, Transient waves generated by a vertical flexible wavemaker plate with a general ramp function, Appl.Ocean Res., 103 (2020). https://doi.org/10.1016/j.apor.2020.102335

[41] Andy's Fluent Theory Guide. ANSYS, Inc., 2021.